

Engineering Substrate Promiscuity of Nucleoside Phosphorylase Via an Insertions–Deletions Strategy

Gaofei Liu, Jialing Wang, Jianlin Chu,* Tianyue Jiang, Song Qin, Zhen Gao, and Bingfang He*



Cite This: *JACS Au* 2024, 4, 454–464



Read Online

ACCESS |

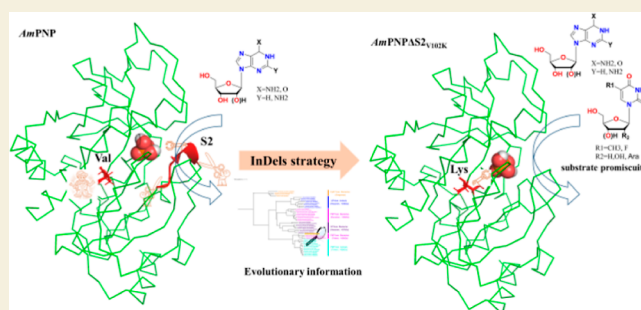
Metrics & More

Article Recommendations

Supporting Information

ABSTRACT: Nucleoside phosphorylases (NPs) are the key enzymes in the nucleoside metabolism pathway and are widely employed for the synthesis of nucleoside analogs, which are difficult to access via conventional synthetic methods. NPs are generally classified as purine nucleoside phosphorylase (PNP) and pyrimidine or uridine nucleoside phosphorylase (PyNP/UP), based on their substrate preference. Here, based on the evolutionary information on the NP-I family, we adopted an insertions–deletions (InDels) strategy to engineer the substrate promiscuity of nucleoside phosphorylase *AmPNP* Δ S_{2V102K}, which exhibits both PNP and UP activities from a trimeric PNP (*AmPNP*) of *Aneurinibacillus migulanus*. Furthermore, the *AmPNP* Δ S_{2V102K} exerted phosphorylation activities toward arabinose nucleoside, fluorosyl nucleoside, and dideoxyribose, thereby broadening the unnatural-ribose nucleoside substrate spectrum of *AmPNP*. Finally, six purine nucleoside analogues were successfully synthesized, using the engineered *AmPNP* Δ S_{2V102K} instead of the traditional “two-enzymes PNP/UP” approach. These results provide deep insights into the catalytic mechanisms of the PNP and demonstrate the benefits of using the InDels strategy to achieve substrate promiscuity in an enzyme, as well as broadening the substrate spectrum of the enzyme.

KEYWORDS: nucleoside phosphorylase, substrate promiscuity, insertions-deletions, evolutionary information, purine nucleoside analogues



INTRODUCTION

Nucleoside phosphorylases (NPs) are essential for the salvage and catabolism of nucleosides in all organisms. They catalyze the reversible phosphorolysis of nucleosides and their analogues in the presence of phosphate. Purine nucleoside phosphorylase (PNP, EC 2.4.2.1) is the largest subfamily of the NP-I family with a preference for purine nucleosides as its substrates.¹ Other members of the NP-I family include uridine phosphorylase (UP, EC 2.4.2.3), which prefers uridine and its analogues to produce uracil and ribose-1-phosphate.¹ Pyrimidine NPs (PyNP, EC 2.4.2.2) belong to the NP-II family and have a substrate preference for pyrimidine nucleosides.¹ NPs are effective biocatalysts for the synthesis of nucleoside drugs.^{2–5} They were used to directly convert the 1-phosphoribose sugar to the nucleoside in a single step, such as islatravir,⁶ molnupiravir⁴ and didanosine⁷ (Scheme 1a). However, 1-phosphoribose sugar is difficult to store because it is easily decomposed.⁸ Also, the phosphate hydrolysis process of purine nucleosides is more thermodynamically favorable for the synthesis of nucleosides, while the phosphate hydrolysis process of pyrimidine nucleosides is the opposite.⁸ To efficiently synthesize purine nucleoside drugs with a high yield, PNP and PyNP or UP have usually been combined in a “one-pot, two-enzymes” reaction system (Scheme 1b).^{2,3} Interestingly, both PNP and UP are members of the NP-I

family with a common α/β -subunit fold and similar monomer structure and catalytic mechanism, but completely different substrate preferences.¹ There are two reported PNP with activity toward both purine nucleosides and pyrimidine nucleosides, but they show very low activity toward pyrimidine nucleosides.^{8,9} Therefore, in this study, we aimed to engineer substrate promiscuity of NP with both PNP and UP activity to reduce the loss of unstable intermediate ribose phosphate in the synthesis of purine nucleoside analogues (Scheme 1b).

The development of strategy for engineering substrate promiscuity in enzymes is very useful and meaningful; it not only broadens the practical applications of biocatalysts in biotechnology, but also contributes to a deeper understanding of enzyme catalytic mechanisms and their evolutionary significance.^{10,11} Many studies were focused on the improving of enzymatic functions by using site substitution in the active pocket region of enzymes or by introducing random mutations of into enzymes.^{12,13} However, in addition to amino acid

Received: September 29, 2023

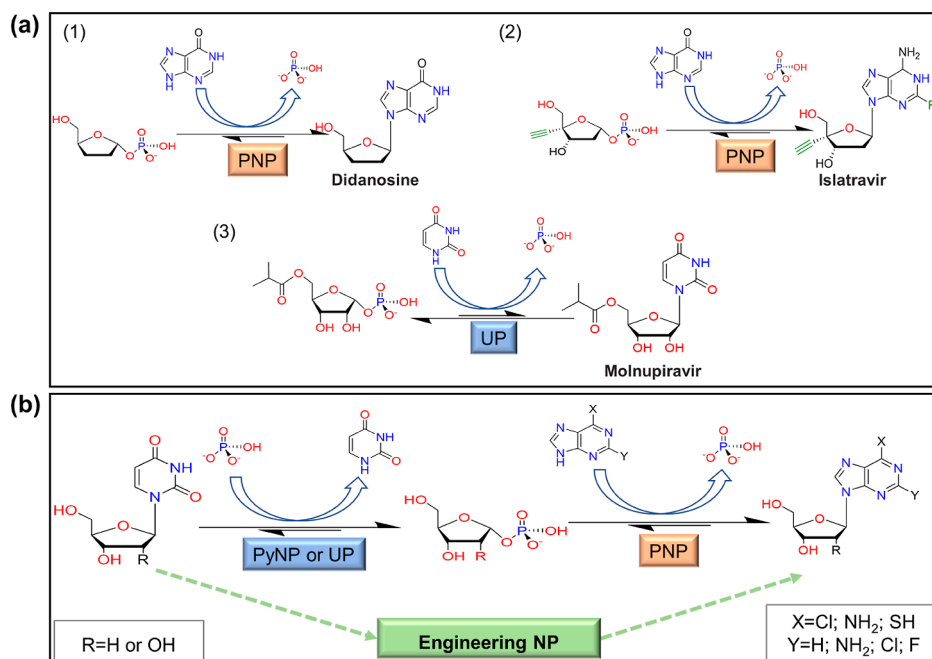
Revised: December 27, 2023

Accepted: January 2, 2024

Published: January 13, 2024



Scheme 1. Synthesis of Nucleoside Analogues via NPs



(AAs) substitutions, insertions–deletions (InDels) may play a more important role in natural and artificial protein evolution.^{14–19} Nevertheless, the role of InDels in shaping enzyme function is still largely unexplored. The main reason is that InDels are approximately 100 times more likely to have a deleterious effect than substitutions leading to the complete inactivation of the enzyme.^{20,21} InDels of AA fragments often occur during the natural evolution of enzymes. Therefore, utilizing the evolutionary information on enzymes to develop an InDels strategy to access substrate promiscuity of enzymes has great potential.

Although members of the same enzyme family usually share key active site residues in a common fold, they have acquired different substrate preferences during natural evolution.^{22,23} Based on the substrate preference and evolutionary information on enzymes, many strategies have been developed to create enzymes with new functions or altered substrate preferences.²⁴ For example, using protein engineering, Gaucher et al. designed a DNA polymerase with the ability to polymerize nonstandard nucleosides, guided by the reconstructed evolutionary adaptation path (REAP).²⁵ This method relies on the phylogenetic analysis of homologous sequences with ancient enzymes having lower substrate specificity to detect characteristics of functional divergence and reconstruct individual mutations along the divergent phylogenetic branches of these functions. Notably, to date, all studies have focused on application of REAP for enzyme engineering using only single or a few AA substitutions. However, in a family member with a low degree of sequence similarity, this method would not be applicable. To further improve this method strategy, we explored an InDels AA fragment as the evolutionary node to obtain target-engineering enzymes.

In this work, we began with the trimeric PNP (*Am*PNP) from *Aneurinibacillus migulanus* AM007²⁶ to shape an engineering NP with a broad substrate spectrum. The analysis of the possible evolution path of the NP-I family and the sequence alignment of bacterial-derived trimeric PNPs and bacterial-derived UPs (with low sequence identity) indicated

that the divergence of the nucleoside phosphorylase function was due to the insertion and deletion of fragments. We then constructed a mutant library of *Am*PNP using the InDels strategy. After screening and reshaping the active site, we obtained an engineering NP (*Am*PNP Δ S2_{V102K}) with both PNP and UP activities. Activities toward arabinose nucleoside, fluorosyl nucleoside, and dideoxynucleoside of the mutant *Am*PNP Δ S2_{V102K} were also detected. We found that the S2 fragment played an important role in the evolution of the substrate preference for NP. In this study, we synthesized several purine nucleoside analogues, using a single enzyme *Am*PNP Δ S2_{V102K}, instead of the “double-enzymes of PNP and NP” for the first time. These results reveal that the introduction of the InDels strategy can lead to substrate promiscuity in protein engineering.

RESULTS

InDels-Designed Library of *Am*PNP

We first constructed a phylogenetic tree of the NP-I family enzymes (Figure 1a). Then, based on their subunit molecular weights and quaternary structures, we proposed an evolutionary pathway between PNPs and UPs (Supporting Information Figure S1). According to the evolutionary pathway analysis of the NP-I family, the occurrence of duplication events might be the main reason for the substrate preference of the NP-I family. Rare bacterial-derived trimeric PNPs were retained during NP-I family evolution. We speculated that these PNPs were closer to their ancestral enzymes, making it easier for them to be shaped into engineering enzymes with substrate promiscuity. Although bacterial-derived UPs have a substrate preference for uridine, they have similar monomer molecular weights, common folds, and catalytic mechanisms as bacterial-derived trimeric PNPs. Therefore, we performed multiple sequence alignment of bacterial-derived UPs and bacterial-derived trimeric PNP. Although UPs and PNPs had low sequence identity (Figure S2a), the secondary structures and monomer structures of UPs

Table 1. Activity of *AmpNP* and Mutants Toward Various Substrate^a

Enzymes	Specific activity (U/mg)					
	purine nucleosides			uridine and its analogues		
	 inosine	 guanosine	 2'-deoxyguanosine	 uridine	 2'-deoxyuridine	 5-methyluridine
<i>AmpNP</i>	79.1±2.3	53.7±3.1	15.5±0.9	ND	ND	ND
<i>AmpNP</i> ::32EK	30.8±1.2	9.3±1.7	5.6±0.5	ND	ND	ND
<i>AmpNP</i> Δ141G	62.2±2.6	98.5±2.0	51.6±2.6	ND	ND	ND
<i>AmpNP</i> Δ151FP	0.9±0.2	0.7±0.03	0.5±0.01	ND	ND	ND
<i>AmpNP</i> Δ233N	ND	ND	ND	ND	ND	ND
<i>AmpNP</i> ΔS2	1.6±0.3	1.0±0.1	1.0±0.1	0.1±0.04	0.02±0.0	<0.01
<i>AmpNP</i> ΔS4	0.8±0.01	0.4±0.01	0.07±0.01	ND	ND	ND
<i>AmpNP</i> ::S5	1.0±0.2	1.2±0.2	1.9±0.2	ND	ND	ND
<i>AmpNP</i> ΔS2 _{V102H}	0.3±0.01	0.2±0.2	0.2±0.03	0.02±0.0	<0.01	<0.01
<i>AmpNP</i> ΔS2 _{V102R}	9.1±1.0	5.5±0.7	5.0±0.8	3.6±1.0	1.2±0.2	0.5±0.02
<i>AmpNP</i> ΔS2 _{V102K}	8.7±1.2	4.3±1.0	5.0±1.3	10.1±1.3	4.8±1.3	4.0±1.9

^aOne enzymatic unit of activity was defined as the amount of enzyme required to convert 1.0 μmol of nucleoside per minute at 50 °C and at pH of 8.0 in 10 mM Na₂HPO₄/KH₂PO₄ buffer. Data are represented as mean ± SD (*n* = 3). Product formation was analyzed by HPLC. HPLC analysis of *AmpNP*ΔS2 activity toward uridine and its analogues were in Supporting Information Figure 1d. ND: not detected.

with those of the WT. We docked the substrates into *AmpNP* and mutant *AmpNP*Δ141G, respectively, and it can be observed from Figure 2a that the structure of the whole

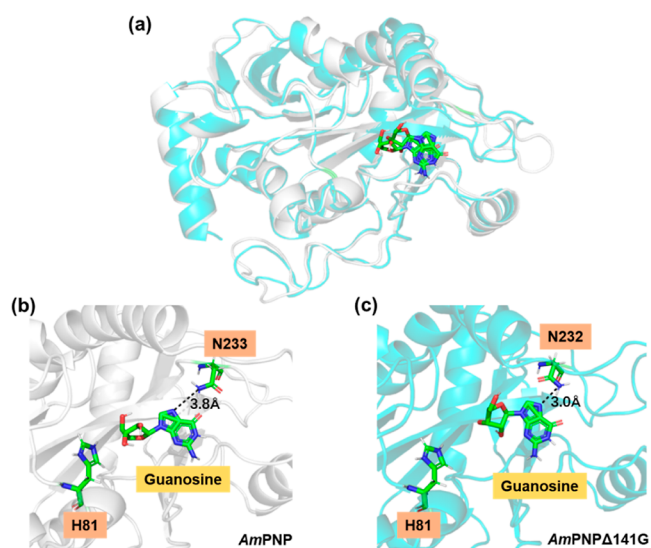


Figure 2. (a) Comparisons of the monomer structures of WT *AmpNP* (white) and *AmpNP*Δ141G (cyans) docking with guanosine. 3D homology models of the *AmpNP* and *AmpNP*Δ141G were conducted using the RoseTTAFold. (b) Molecular docking of guanosine into *AmpNP*. (c) Molecular docking of guanosine into *AmpNP*Δ141G. The black dotted line represents the distance between the N atoms of N233/N232 and N7 of the purine base.

protein was slightly changed due to the deletion of 141G. In *AmpNP* (Figure 2b), residue N233 provides a proton to N7 of the base of guanosine, which allows the formation of a hydrogen bond between the given atom and the enzyme. Electron flow from the ribose stabilizes the resulting electron pull of the base. In *AmpNP*Δ141G (Figure 2c), this hydrogen bonding distance between N232 and the guanosine's purine base N7 is shorter, promoting the transfer of protons to the N7 of the purine base, stabilizing the negative charge formed on the base in the transition state, and thus increasing the phosphorylation activity of the enzyme on guanosine.

Reshaping the Binding Pocket of Mutant *AmpNP*ΔS2

To improve the phosphorylation activity of mutant *AmpNP*ΔS2, we further engineered it by reshaping its binding pocket. Our structural comparison analysis results (Figure S7) revealed that the low activity of *AmpNP*ΔS2 resulted from the deletion of the key AA residue H81, which develops electrostatic strain during the deprotonation of the phosphate monoanion to the dianion (H81-PO₄⁼) to initiate a nucleophilic attack on the ribosyl group in the reversible phosphorolysis of nucleosides (Figure 3a).²⁷ Although the NPs of the NP-I family have similar structures and catalytic mechanisms, the catalytic residues and positions for deprotonation of the phosphate monoanion are different (*AmpNP*: H81 and *EcUP*: R91)²⁸ (Figure 3b). The position of this residue is absent in *AmpNP*ΔS2, but the position (V102) corresponding to residue R91 in *EcUP* is present in the mutant *AmpNP*ΔS2 (Figure 3c). Therefore, residue V102 in *AmpNP*ΔS2 was replaced by an alkaline AA (H, R, and K)

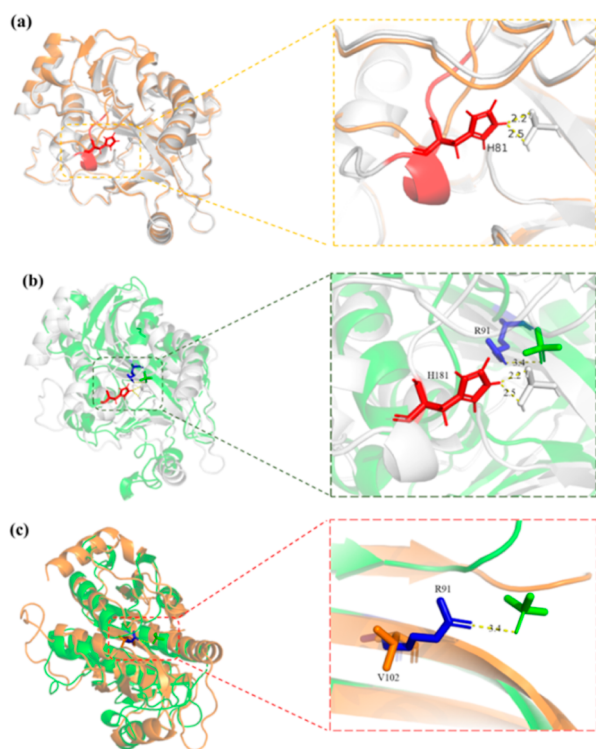


Figure 3. Comparisons of the monomer structures of WT *AmpNP* (white), mutant *AmpNP* Δ S2 (orange), and *EcUP* (green, pdb ID: 1rxs). 3D homology models of the *AmpNP* and *AmpNP* Δ S2 were conducted using the RoseTTAFold (<https://rosetta.bakerlab.org/>) with 4m1e (PDB accession code of PNP from *Planctomyces limnophilus* DSM 3776) as a template, which has 48.33% protein sequence identities with *AmpNP*. (a) Comparison of the monomer structures of *AmpNP* and *AmpNP* Δ S2. The S2 fragment is displayed in red. (b) Comparison of the monomer structure of *AmpNP* and *EcUP*. The key AA residues for the deprotonation of phosphate ions are H81 (*AmpNP*) and R91 (*EcUP*), respectively. (c) Comparison of the monomer structure of *EcUP* and *AmpNP* Δ S2. The AA residues V102 in *AmpNP* Δ S2 correspond with the AA residue R91 in *EcUP*.

to reshape the binding pocket. The phosphorylation activities of the obtained mutants (*AmpNP* Δ S2_{V102H}, *AmpNP* Δ S2_{V102R}, and *AmpNP* Δ S2_{V102K}) were tested by using inosine and uridine as substrates. As seen in Table 1, the phosphorylation activities of the mutants *AmpNP* Δ S2_{V102R} and *AmpNP* Δ S2_{V102K} toward inosine were 5.77-folds and 5.55-folds higher, respectively, and the phosphorylation activity toward uridine were 29.83-folds and 83.75-folds higher,

respectively, than those of *AmpNP* Δ S2. The mutant *AmpNP* Δ S2_{V102K} showed the highest activity toward inosine and uridine.

To investigate the possible catalytic mechanism of mutant *AmpNP* Δ S2_{V102K}, structural models of *AmpNP*, *AmpNP* Δ S2, and *AmpNP* Δ S2_{V102K} were established and then docked with phosphate ions using AutoDock (Figure 4). As depicted in Figure 4a, residue H81 of the WT *AmpNP* forms hydrogen bond contacts with the phosphate ion, stabilizing the phosphate in the active pocket and positioning it favorably for deprotonation. Due to the deletion of the S2 fragment containing the residue H81, the mutant *AmpNP* Δ S2 lacks a suitable residue in the corresponding position to stabilize and deprotonate the phosphate ion. Consequently, the activation of the phosphate ion and the subsequent nucleophilic attack on the nucleoside are hindered, leading to a considerable reduction in its phosphorylation ability. However, the AA H59 in the active pocket can form a weak hydrogen bond with the phosphate ion in the absence of H81 to deprotonate the phosphate ion and complete the phosphorolysis reaction by nucleophilic attack on the nucleoside (Figure 4b). Subsequently, residue V102 K was introduced into the mutant *AmpNP* Δ S2_{V102K}, allowing the formation of a hydrogen bond with the phosphate ion (Figure 4c). Thus, the stabilization and deprotonation of the phosphate ion and the subsequent nucleophilic attack on the nucleoside were successfully completed, increasing the phosphorylation activity of the mutant. The change in the binding energy of *AmpNP* and its mutants to the phosphate ion was also consistent with this process. The possible *AmpNP* Δ S2_{V102K} catalytic process is presented in the Supporting Information Figure S5.

Performance Analysis of *AmpNP* and Its Variants

Furthermore, the phosphorylation activities of WT *AmpNP* and its mutants toward purine and pyrimidine nucleosides were tested (Table 2). *AmpNP* displayed a substrate preference for purine nucleosides but exhibited no phosphorylation activity for arabinopurine nucleosides. The mutant *AmpNP* Δ S2_{V102K} exhibits phosphorylation activity toward both purine nucleosides and uridine. Thus, mutant *AmpNP* Δ S2_{V102K} showed phosphorylation activity characteristic of both PNPs and UPs. In addition, the mutant *AmpNP* Δ S2_{V102K} also exerted phosphorylation activity toward some base-modified uridines, such as 5-methyluridine and 5'-fluoro-2'-deoxyuridine. The change in the substrate promiscuity of *AmpNP* Δ S2_{V102K} was observed not only in its base but also in its ribose group. For instance, it has phosphorylation

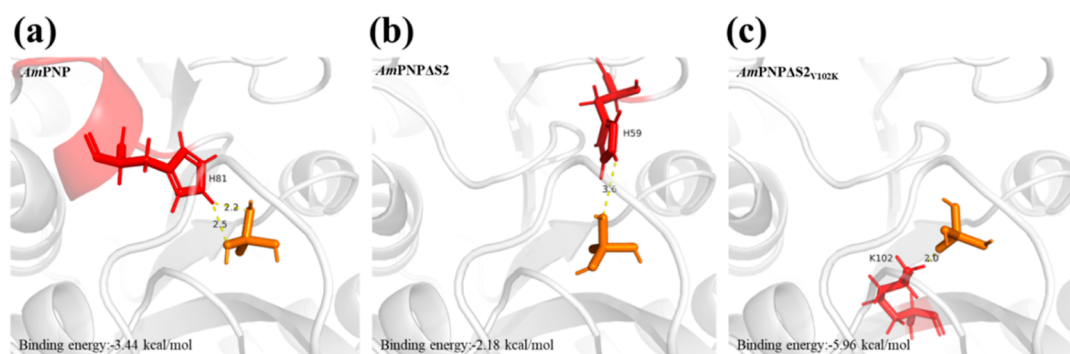
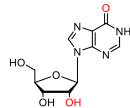
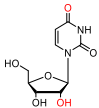
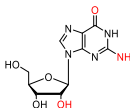
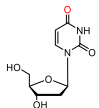
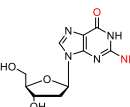
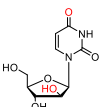
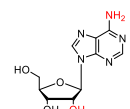
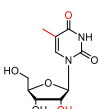
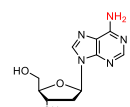
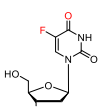
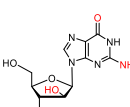
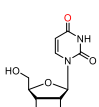
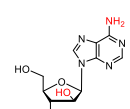
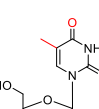
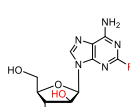
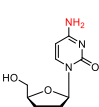
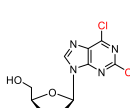
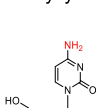


Figure 4. (a) Molecular docking of phosphate ions into *AmpNP*. (b) Molecular docking of phosphate ions into *AmpNP* Δ S2. (c) Molecular docking of phosphate ions into *AmpNP* Δ S2_{V102K}. The hydrogen bond is the yellow dotted line.

Table 2. Phosphorylation Activity of WT and *AmPNPΔS2_{V102K}* Toward Purine Nucleosides and Pyrimidine Nucleosides^a

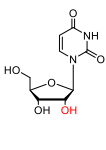
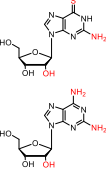
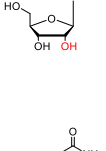
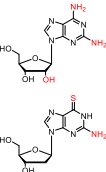
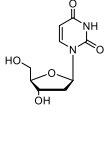
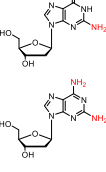
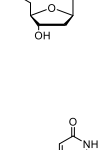
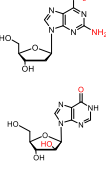
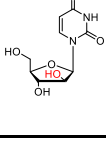
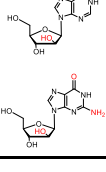
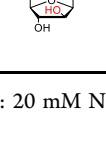
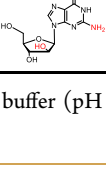
	Specific activity (U/mg)			Specific activity (U/mg)	
	WT	<i>AmPNPΔS2_{V102K}</i>		WT	<i>AmPNPΔS2_{V102K}</i>
 inosine	79.3±2.0	8.7±1.2	 uridine	ND	10.1±1.3
 guanosine	53.7±1.3	13.0±0.9	 2'-deoxyuridine	ND	4.2±0.5
 2'-deoxyguanosine	16.6±2.0	9.9±1.1	 arabinofuranosyluracil	ND	1.3±0.04
 adenosine	2.6±0.8	0.2±0.01	 5-methyluridine	ND	7.7±0.9
 2'-deoxyadenosine	ND	0.04±0.01	 5'-fluoro-2'-deoxyuridine	ND	1.6±0.3
 arabinosylguanine	ND	0.1±0.02	 2'-deoxy-2'-fluorouridine	ND	1.9±0.3
 vidarabine	ND	ND	 stavudine	ND	1.3±0.1
 fludarabine	ND	<0.01	 2'-deoxycytidine	ND	ND
 2,6-dichloropurine nucleoside	ND	ND	 cytidine	ND	ND

^aND: not detected.

activity toward arabinosylguanine, arabinofuranosyluracil, 2'-deoxy-2'-fluoridine, and stavudine (dideoxyribonucleoside). These results indicated that the mutant *AmPNPΔS2_{V102K}* had activities toward a broad substrate spectrum. Moreover, the mutant *AmPNPΔ141G* significantly enhanced the activity toward guanosine and 2'-deoxyguanosine (Supporting In-

formation Table S2). Finally, a combinatorial mutant (*AmPNPΔS2_{V102K}Δ141G*) was constructed, which showed higher phosphorylation activity for guanosine and deoxyguanosine than that of *AmPNPΔS2_{V102K}* (Supporting Information Table S2).

Table 3. Biosynthesis of Purine Nucleoside Analogues by *AmPNP*ΔS₂V₁₀₂K^a

Pentofuranosyl Donor	Purine base	Products	Ribosylation (%)		
			<i>AmPNP</i> & <i>BbPyNP</i>	<i>AmPNP</i> ΔS ₂ V ₁₀₂ K	
			92.0	ND	82.4
			98.3	ND	46.7
			89.3	ND	60.6
			96.5	ND	21.7
			ND	ND	10.9
			ND	ND	6.5

^aTemperature: 50 °C. Medium: 20 mM Na₂HPO₄/KH₂PO₄ buffer (pH 7.5). Substrates: pentofuranosyl donor: Purine base. 10:5 mM. Reaction time: 12 h. ND: not detected.

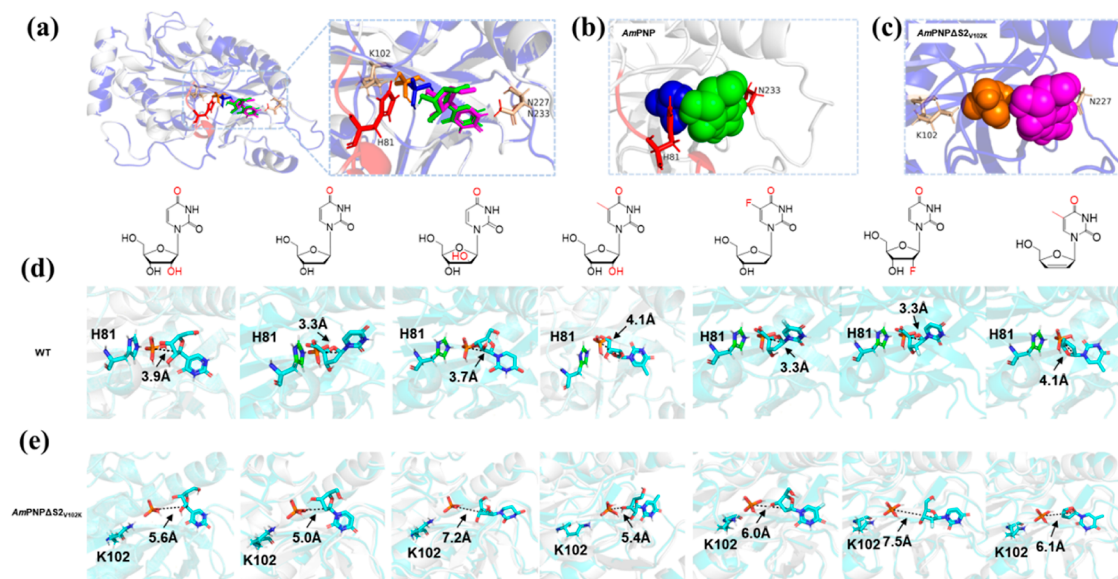


Figure 5. Molecular docking of *AmPNP* and *AmPNP*ΔS₂V₁₀₂K with substrates. (a) Comparison of docking results of *AmPNP* (white) and *AmPNP*ΔS₂V₁₀₂K (blue) with phosphate ions and uridine. (b) Molecular docking of *AmPNP* with substrate phosphate ions (blue) and uridine (green). (c) Molecular docking of *AmPNP*ΔS₂V₁₀₂K with substrates phosphate ions (orange) and uridine (magenta). (d) Comparison of docking results of *AmPNP* (white) with phosphate ions and *AmPNP* (cyans) with pyrimidine nucleoside (uridine, 2'-deoxyuridine, arabinofuranosyluracil, 5-methyluridine, 5'-fluoro-2'-deoxyuridine, 2'-deoxy-2'-fluridine and stavudine). (e) Comparison of docking results of *AmPNP*ΔS₂V₁₀₂K (white) with phosphate ions and *AmPNP*ΔS₂V₁₀₂K (cyans) with pyrimidine nucleoside (uridine, 2'-deoxyuridine, arabinofuranosyluracil, 5-methyluridine, 5'-fluoro-2'-deoxyuridine, 2'-deoxy-2'-fluridine, and stavudine). The black dotted line represents the distance between the P atom of the phosphate ion and the C1 position on the nucleoside sugar base.

Figure S6 (Supporting Information) displays data of the effects of pH and temperature on the activity and stability of the WT *AmPNP* and its mutant *AmPNP*ΔS₂V₁₀₂K. Both *AmPNP* and *AmPNP*ΔS₂V₁₀₂K maintained nearly 100% of their initial activities at 50 °C. However, at 60 °C, the stability of mutant *AmPNP*ΔS₂V₁₀₂K decreased rapidly. We speculate that the S2 fragment is crucial for the enzyme's thermostability.

This result may suggest that the insertion of S2 fragment in the evolutionary process contributed not only to enhancing the substrate preference of the NP-I family for specific nucleosides, but also to increasing the enzyme's thermostability. The highest phosphorolysis activity of *AmPNP* was observed at a pH of 7.5, while the optimal pH for *AmPNP*ΔS₂V₁₀₂K was 8.0. These differences may be attributed to changes in the AA

residues (H81 in *AmPNP* and K102 in *AmPNP* Δ S2_{V102 K}) that deprotonate the phosphate ion during the phosphorylation reaction.

We also tried to synthesize purine nucleoside analogues using the purified single enzyme *AmPNP* Δ S2_{V102 K}, instead of the “one-pot, two-enzymes” method (Scheme 1b). Subsequently, six purine nucleoside analogues were successfully synthesized with a yield ranging from 6.54 to 82.36% (Table 3). Hence, it can be concluded that the mutant *AmPNP* Δ S2_{V102 K} is capable of synthesizing not only purine nucleosides and deoxynucleosides but also purine arabinosides, indicating that this mutant has a significant potential for the biosynthesis of purine nucleoside analogs. Given that NP reactions are under thermodynamic control, even enzymes that display low-level promiscuous activity toward a given nucleobase can form the corresponding nucleoside at appreciable levels when equilibrium is reached.⁸

Molecular Dynamics Illustrate Substrate Promiscuity of *AmPNP* Δ S2_{V102 K}

We performed molecular dynamics (MD) simulations to further elucidate the molecular basis of substrate promiscuity in *AmPNP* Δ S2_{V102 K}. We ran 50 ns simulations of *AmPNP* and *AmPNP* Δ S2_{V102 K} bound to phosphate ions and uridine. Using the initial structure as a template, we analyzed the root-mean-square deviation (RMSD) for all C α atoms through a trajectory of approximately 50 ns for each system (Supporting Information Figure S7). Based on the MD simulation results, we determined the average structures were determined from the trajectories.

When comparing the docking results of *AmPNP* and *AmPNP* Δ S2_{V102 K} with those of uridine and phosphate ions (Figure 5a), we found that the spatial positions of uridine almost overlapped, whereas the positions of phosphate ions were significantly different. In *AmPNP* (Figure 5b), the spaces occupied by the phosphate ion and uridine overlapped. This indicates that substrates (uridine and phosphate ions) cannot be present at the active center at the same time, resulting in no catalytic activity of WT for uridine. In the mutant *AmPNP* Δ S2_{V102 K} (Figure 5c), the deletion of H81 and the introduction of a new catalytic residue K102 changed the position of phosphate ions and the strong hydrogen bond formed by K102 to phosphate ions increased the distance between phosphate ions and uridine. This allows both uridine and phosphate ions to be present in the active center simultaneously to complete the phosphorylation reaction. Similar to the STR enzyme, both tryptamine and secologanin substrates are clearly arranged in close vicinity but do not overlap.

To verify this interpretation, we also present the results of docking *AmPNP* and *AmPNP* Δ S2_{V102 K} with other pyrimidine nucleosides, including 2'-deoxyuridine, arabinofuranosyluracil, 5-methyluridine, 5'-fluoro-2'-deoxyuridine, 2'-deoxy-2'-fluridine, and stavudine. The distance between the P atom of the phosphate ion and the C1 position on the nucleoside sugar base (P–C1) was calculated after structural alignment. It was found that in *AmPNP*, the distances of P–C1 ranged from 3.3 to 4.1 Å, and the shorter distances prevented the simultaneous presence of two substrates in the active center (Figure 5d). However, in the mutant *AmPNP* Δ S2_{V102 K}, these distances of P–C1 were increased to 5.0–7.1 Å, ensuring a sufficient spatial position to allow the simultaneous presence of both substrates

within the active center to complete the phosphorylation reaction (Figure 5e).

DISCUSSION

The present work validates a strategy for creating an engineering NP with substrate promiscuity based on InDels fragments of natural evolution. Initially, our intention was to use the REAP strategy to create an engineered NP with PNP and UP phosphorylation activities. However, to date, all studies have focused on REAP for enzyme engineering using only single or a few AA substitutions.^{24,25} In the case of a low PNP and UP sequence similarity (<20%), the established mutant library capacity through the REAP strategy was too large to be fully experimentally verified. Thus, based on the previously reported analysis of evolution path of the NP-I family,¹ we presumed that a common ancestor of the NP-I family may have accepted purine nucleosides and uridine substrates. Then, major InDels occurred over time, resulting in an increased substrate preference of the NP-I family members. Inspired by REAP, we expected to develop an InDels strategy to create an engineered NP with substrate promiscuity guided by existing evolutionary information. The InDels strategy for the modification of enzyme functions has been recently proposed.^{17–19} In contrast, the role of InDels in creating an engineering NP with substrate promiscuity is still unexplored.

In this study, the rare bacterial-derived trimeric *AmPNP* was selected as a backbone because it is closer to ancestral enzymes and easier to be shaped into an engineered NP with substrate promiscuity. From the InDels-designed *AmPNP* mutant library, we screened mutant *AmPNP* Δ S2, which showed phosphorylation activity toward inosine (substrate of PNP) and uridine (substrate of UP). This suggests that the insertion of S2 fragment is an important evolutionary node in the NP-I family. Since then, there has been a PNP enzyme whose substrate preference is to purine nucleoside. This also suggests that some ancestral enzymes diverged in substrate preference during evolution through the InDels of characteristic fragment nodes.¹⁶

Based on the catalytic mechanism of the NP-I family, we reshaped the binding pocket of mutant *AmPNP* Δ S2. By introducing an alkaline AA into the active pocket to replace the H in Δ S2, we successfully achieved completed stabilization and deprotonation of the phosphate ion and the subsequent nucleophilic attack on the nucleoside. In addition, the mutant *AmPNP* Δ S2_{V102 K} Δ 141G significantly increased the activity of guanosine and 2'-deoxyguanosine. This result indicates that the phosphorylation activity of engineered NP with substrate promiscuity toward nucleosides can be further improved through protein engineering. The S2 fragment (the catalytic residue H81 in the S2 fragment) was deleted in the mutant *AmPNP* Δ S2, significantly reducing its natural catalytic activity. Subsequently, an engineered NP with substrate promiscuity was obtained by reshaping the active pocket.

The *AmPNP* Δ S2_{V102 K} was obtained via protein engineering guided by the InDels strategy, although its activity was still not satisfactory. However, it is encouraging that *AmPNP* Δ S2_{V102 K} exhibited phosphorylation activity not only toward different-base nucleoside substrates but also toward ribose-modified nucleoside substrates. The obtained engineered NP appears to be consistent with the substrate promiscuity of presumed ancestor enzymes.¹ The development of nucleoside drugs is changing rapidly, with various nucleoside compounds being created^{29,30} quickly. Modifying the nucleoside phosphorylase

with strong nucleoside substrate specificity to synthesize new nucleoside analogues seems to require more tedious work because existing NPs have evolved to adapt to specific substrates. Conversely, using *AmPNP* Δ S_{2-V102K} as a starting template for NP evolution, increasing its activity for specific nucleoside analogs from different evolutionary paths, and achieving high catalytic activity for specific nucleosides represents a greater possibility. This is also the first report of using a single NP with phosphorylation activity in both PNP and UP to convert uridine and its analogues into purine nucleosides analogues. This discovery facilitates the development of substrate promiscuity in NPs to meet the simple operation of nucleoside analogue biosynthesis with different strategies. This InDels strategy, combined with REAP, also has a potential practical application value in the construction of engineered enzymes with substrate promiscuity because the mutant library that needs to be constructed is small.

CONCLUSIONS

In summary, we have developed an InDels strategy for substrate promiscuity of enzyme. The approach suggested here differs from mainstream protein engineering methods (AAs substitution). It proposes the deletion or insertion of characteristic enzyme fragments based on evolutionary information analysis, which is more suitable for altering the substrate preference of an enzyme. We developed a multi-functional NP using the InDels strategy and obtained a mutant with relatively high phosphorylation activities by reshaping its binding pocket. The mutant not only has the potential to serve as an excellent catalyst for the synthesis of purine nucleoside analogue but also expands the existing understanding of the natural evolutionary mechanism of PNP. In brief, the InDels strategy is a method for designing and creating novel functional enzymes.

EXPERIMENTAL METHODS

Plasmids, Strains, and Chemicals

Nucleosides and purine bases and chemicals of analytical grade were purchased from Aladdin (Shanghai, China). The solvents used for high-performance liquid chromatography (HPLC) were of HPLC grade. The plasmid utilized in this work was pET28a (+)-*AmPNP*, which contained the PNP gene from the strain *A. migulanus* AM007 (locus: AYW33784). The strain *E. coli* BL21(DE3), employed for protein expression examinations, was obtained from Novagen (USA). The restriction enzymes were purchased from Takara (Japan).

Construction of Phylogenetic Trees, Sequences Alignment, and Mutant Library Design

The AA sequences of the NP-I family from different species were obtained from the National Center for Biotechnology Information database (<https://www.ncbi.nlm.nih.gov/>). Phylogenetic trees of the protein sequences were then developed by using Mega 11 software and the neighbor-joining method. Sequence analysis showed that trimeric and hexameric PNPs from bacteria as well as hexameric UPs from bacteria were highly conserved. Thus, we selected four trimeric PNPs sequences from bacteria and four hexameric UPs sequences from bacteria to construct the alignment of multiple sequences, which was performed with ClustalX 2.1.

The sequence alignment results revealed the region where UP and PNP differed in the number of AAs. Then, the AA sequence of *AmPNP* was used as the initial template to construct a small mutant library. This library included four mutants with the deletion of long AA fragments and one mutant with the insertion of a longer AA fragment, as well as five mutants with the insertion and deletion of short AAs fragments.

Construction of Plasmids and Mutagenesis

The plasmid pET28a-*AmPNP* (*NheI*-*Bam**HI* restriction sites) was utilized as the template for mutagenesis. Site-directed mutagenesis was performed by whole-plasmid amplification (for short AA fragments) or overlap extension PCR (for long AA fragments). The primers used in this study were designed as described in the Supporting Information (Table S3). The mutations were confirmed by nucleotide sequencing, and the recombinant plasmid was transformed into *E. coli* BL21 (DE3) competent cells. Every engineered *AmPNP* variant was fused to a 6*histidine tag at the N-terminus to facilitate easy purification via affinity chromatography.

Purification of *AmPNP* and Its Mutants

The solution with the recombinant protein with an N-terminal 6*His-tag of *AmPNP* and its mutants was obtained by previously described methods 2. It was then purified with a HisTrap FF column (GE Healthcare, Fairfield, USA) according to the manufacturer's manual. Then, the mutants were further purified to avoid background contamination by using gel-filtration chromatography on a Superdex 200 Increase 10/300 GL column (GE Healthcare, Buckinghamshire, UK). An ÄKTA pure system and a column Superdex 200 Increase 10/300 GL were used. The standard proteins and the purified mutant samples were dissolved in the buffer (0.01 M phosphate buffer, 0.14 M NaCl, pH 8.0) with a final concentration of 2 mg/mL. For analysis, a flow rate of 0.5 mL/min and an injection volume of 0.5 mL were set. The apparent molecular weight of the purified enzymes was estimated on 12% SDS-PAGE gel. The concentration of the purified proteins was measured using the bicinchoninic acid (BCA) Protein Assay Kit (Zhongke Ruitai, Biological Technology Co., Ltd., Beijing, China).

Determination of Enzymatic Activity and Substrate Specificity

The phosphorolysis activity of the WT *AmPNP* and its variants was determined as previously described.²⁶ The nucleoside substrates tested contained purine nucleosides (inosine, guanosine, 2'-deoxyguanosine, arabinosylguanine, adenosine, 2'-deoxyadenosine, vidarabine, fludarabine, and dichloropurine nucleoside) and pyrimidine nucleosides (uridine, 2'-deoxyuridine, arabinofuranosyluracil, cytidine, 2'-deoxycytidine, 5-methyluridine, 5'-fluoro-2'-deoxyuridine, 2'-deoxy-2'-fluridine, and stavudine). One enzymatic unit of activity was defined as the amount of enzyme required to convert 1.0 μ mol of nucleoside per minute at 50 °C and at pH 8.0 in 10 mM Na₂HPO₄/KH₂PO₄ buffer.

Homology Modeling and Substrate Docking Simulation

3D homology modeling of the *AmPNP* and its mutants was conducted using the RoseTTAFold (<https://rosetta.bakerlab.org/>) with 4m1e (PDB accession code of PNP from *P. limnophilus* DSM 3776) as a template, which has 48.33% protein sequence identities with *AmPNP*, and illustrated as cartoon diagrams using PyMOL 2.5. The putative catalytic key AA of *AmPNP* was selected from the superimposed structure with 4m1e and the substrate binding site was selected from the model structure. In addition, the coordinates of the phosphate substrate were manually generated and energetically optimized using the MM2 force field with Chem3D Ultra 8.0. AutoDock (version 4.2)³¹ was applied to the docking of phosphate into the binary homology model of *AmPNP* by assigning H81 or K102 as a grid center. Among the 256 docking poses generated from docking simulations, the one with the minimum docking energy value was selected.

All MD simulations were performed with the GROMACS software package (version 5.1.0) using the GROMOS96 force field at 300 K and 1 atm in a water solvent system for 50 ns. Additional details have been described previously.³² The GROMACS tool was used to analyze the trajectories. The RMSD values were computed using *g_rms*. The RMSD of all simulations is displayed in the Supporting Information Figure S9. The PyMOL package was used to generate and view the molecular graphics.

Characterization of AmPNP and Its Mutants

The effects of pH and temperature on the activity of AmPNP Δ S2 and AmPNP Δ S2_{V102K} were determined using inosine as the substrate under the conditions described above. The pH of reactions varied from pH 6.0 to 9.0, and the reaction temperatures ranged from 30 to 75 °C. The pH stability was evaluated under the same conditions; the enzyme was incubated for 3 h in different buffers. The thermostability of AmPNP Δ S2 and AmPNP Δ S2_{V102K} was determined by measuring the residual activity at temperatures ranging from 30 to 65 °C after the enzyme had been incubated for 3 h.

Biosynthesis of Purine Nucleoside Analogues Via AmPNP Δ S2_{V102K}

Transglycosylation reactions were performed with AmPNP Δ S2_{V102K} in 20 mM Na₂HPO₄/KH₂PO₄ buffer (pH 7.0) and 50 °C using uridine, 2-deoxyuridine, and arabinofuranosyluracil as ribose donors and purine bases (2,6-diaminopurine, 6-thioguanine and 2-amino-6-chloropurine) as ribose receptors. The reaction mixture was obtained and then analyzed by HPLC to quantitatively determine the reaction products.

ASSOCIATED CONTENT

Supporting Information

The Supporting Information is available free of charge at <https://pubs.acs.org/doi/10.1021/jacsau.3c00581>.

Evolutionary pathway, structure and sequence alignment, SDS-PAGE, catalytic process, biochemical characterization, and RMSD. Sequences information, phosphorylation activity, and primers (PDF)

AUTHOR INFORMATION

Corresponding Authors

Jianlin Chu – School of Pharmaceutical Sciences, Nanjing Tech University, Nanjing 211800, China; orcid.org/0000-0001-8197-6459; Email: cjl2fl@126.com

Bingfang He – College of Biotechnology and Pharmaceutical Engineering, Nanjing Tech University, Nanjing 211800, China; School of Pharmaceutical Sciences, Nanjing Tech University, Nanjing 211800, China; orcid.org/0000-0002-4502-9531; Email: bingfanghe@njtech.edu.cn

Authors

Gaofei Liu – College of Biotechnology and Pharmaceutical Engineering, Nanjing Tech University, Nanjing 211800, China

Jialing Wang – College of Biotechnology and Pharmaceutical Engineering, Nanjing Tech University, Nanjing 211800, China

Tianyue Jiang – School of Pharmaceutical Sciences, Nanjing Tech University, Nanjing 211800, China

Song Qin – School of Pharmaceutical Sciences, Nanjing Tech University, Nanjing 211800, China

Zhen Gao – College of Biotechnology and Pharmaceutical Engineering, Nanjing Tech University, Nanjing 211800, China

Complete contact information is available at: <https://pubs.acs.org/10.1021/jacsau.3c00581>

Author Contributions

G.L. and J.W. contributed equally to this work. J.C. and B.H. designed the project; G.L. and J.W. performed molecular cloning/enzyme assays and conducted bioinformatics analysis;

S.Q. and Z.G. supervised the work; G.L., J.W., and T.J. wrote the manuscript with input from all authors.

Notes

The authors declare no competing financial interest.

ACKNOWLEDGMENTS

This work was supported by the National Key Research and Development Program of China (2018YFA0902000, 2021YFC2101500), the Jiangsu Synergetic Innovation Center for Advanced Bio-Manufacture (NO. XTC2206). We are grateful to High Performance Computing Center of Nanjing Tech University for supporting the computational resources.

REFERENCES

- (1) Pugmire, M. J.; Ealick, S. E. Structural analyses reveal two distinct families of nucleoside phosphorylases. *Biochem. J.* **2002**, *361*, 1–25.
- (2) Zhou, X. R.; Szeker, K.; Jiao, L. Y.; Oestreich, M.; Mikhailopulo, I. A.; Neubauer, P. Synthesis of 2,6-Dihalogenated Purine Nucleosides by Thermostable Nucleoside Phosphorylases. *Adv. Synth. Catal.* **2015**, *357* (6), 1237–1244.
- (3) Serra, I.; Daly, S.; Alcantara, A. R.; Bianchi, D.; Terreni, M.; Ubiali, D. Redesigning the synthesis of vidarabine via a multi-enzymatic reaction catalyzed by immobilized nucleoside phosphorylases. *RSC Adv.* **2015**, *5* (30), 23569–23577.
- (4) McIntosh, J. A.; Benkovics, T.; Silverman, S. M.; Huffman, M. A.; Kong, J.; Maligres, P. E.; Itoh, T.; Yang, H.; Verma, D.; Pan, W. L.; Ho, H. I.; Vroom, J.; Knight, A. M.; Hurtak, J. A.; Klapars, A.; Fryszkowska, A.; Morris, W. J.; Strotman, N. A.; Murphy, G. S.; Maloney, K. M.; Fier, P. S. Engineered Ribosyl-1-Kinase Enables Concise Synthesis of Molnupiravir, an Antiviral for COVID-19. *ACS Cent. Sci.* **2021**, *7* (12), 1980–1985.
- (5) Kaspar, F.; Seeger, M.; Westarp, S.; Köllmann, C.; Lehmann, A. P.; Pausch, P.; Kemper, S.; Neubauer, P.; Bange, G.; Schallmeyer, A.; Werz, D. B.; Kurreck, A. Diversification of 4'-Methylated Nucleosides by Nucleoside Phosphorylases. *ACS Catal.* **2021**, *11* (17), 10830–10835.
- (6) Huffman, M. A.; Fryszkowska, A.; Alvizo, O.; Borra-Garske, M.; Campos, K. R.; Canada, K. A.; Devine, P. N.; Duan, D.; Forstater, J. H.; Grosser, S. T.; Halsey, H. M.; Hughes, G. J.; Jo, J.; Joyce, L. A.; Kolev, J. N.; Liang, J.; Maloney, K. M.; Mann, B. F.; Marshall, N. M.; McLaughlin, M.; Moore, J. C.; Murphy, G. S.; Nawrat, C. C.; Nazor, J.; Novick, S.; Patel, N. R.; Rodriguez-Granillo, A.; Robaire, S. A.; Sherer, E. C.; Truppo, M. D.; Whittaker, A. M.; Verma, D.; Xiao, L.; Xu, Y.; Yang, H. Design of an in vitro biocatalytic cascade for the manufacture of islatravir. *Science* **2019**, *366* (6470), 1255–1259.
- (7) Birmingham, W. R.; Starbird, C. A.; Panosian, T. D.; Nannemann, D. P.; Iverson, T.; Bachmann, B. O. Bioretrosynthetic construction of a didanosine biosynthetic pathway. *Nat. Chem. Biol.* **2014**, *10* (5), 392–399.
- (8) Kaspar, F.; Giessmann, R. T.; Neubauer, P.; Wagner, A.; Gimpel, M. Thermodynamic reaction control of nucleoside phosphorylation. *Adv. Synth. Catal.* **2020**, *362* (4), 867–876.
- (9) Kicska, G. A.; Tyler, P. C.; Evans, G. B.; Furneaux, R. H.; Kim, K.; Schramm, V. L. Transition state analogue inhibitors of purine nucleoside phosphorylase from *Plasmodium falciparum*. *J. Biol. Chem.* **2002**, *277* (5), 3219–3225.
- (10) Renata, H.; Wang, Z. J.; Arnold, F. H. Expanding the Enzyme Universe: Accessing Non-Natural Reactions by Mechanism-Guided Directed Evolution. *Angew. Chem., Int. Ed.* **2015**, *54* (11), 3351–3367.
- (11) Toscano, M. D.; Woycechowsky, K. J.; Hilvert, D. Minimalist active-site redesign: Teaching old enzymes new tricks. *Angew. Chem., Int. Ed.* **2007**, *46* (18), 3212–3236.
- (12) Reetz, M. T.; Carballeira, J. D. Iterative saturation mutagenesis (ISM) for rapid directed evolution of functional enzymes. *Nat. Protoc.* **2007**, *2* (4), 891–903.

- (13) Zheng, W. L.; Yu, H. R.; Fang, S.; Chen, K. T.; Wang, Z.; Cheng, X. L.; Xu, G.; Yang, L. R.; Wu, J. P. Directed Evolution of l-Threonine Aldolase for the Diastereoselective Synthesis of β -Hydroxy- α -amino Acids. *ACS Catal.* **2021**, *11* (6), 3198–3205.
- (14) Chothia, C.; Gough, J.; Vogel, C.; Teichmann, S. A. Evolution of the protein repertoire. *Science* **2003**, *300* (5626), 1701–1703.
- (15) Stavrinides, A.; Tatsis, E. C.; Caputi, L.; Foureau, E.; Stevenson, C. E. M.; Lawson, D. M.; Courdavault, V.; O'Connor, S. E. Structural investigation of heteroyohimbine alkaloid synthesis reveals active site elements that control stereoselectivity. *Nat. Commun.* **2016**, *7*, 12116.
- (16) Toledo-Patiño, S.; Pascarelli, S.; Uechi, G.-i.; Laurino, P. Insertions and deletions mediated functional divergence of Rossmann fold enzymes. *Proc. Natl. Acad. Sci. U.S.A.* **2022**, *119* (48), No. e2207965119.
- (17) Hoque, M. A.; Zhang, Y.; Chen, L. Q.; Yang, G. Y.; Khatun, M. A.; Chen, H. F.; Hao, L.; Feng, Y. Stepwise Loop Insertion Strategy for Active Site Remodeling to Generate Novel Enzyme Functions. *ACS Chem. Biol.* **2017**, *12* (5), 1188–1193.
- (18) Emond, S.; Petek, M.; Kay, E. J.; Heames, B.; Devenish, S. R. A.; Tokuriki, N.; Hollfelder, F. Accessing unexplored regions of sequence space in directed enzyme evolution via insertion/deletion mutagenesis. *Nat. Commun.* **2020**, *11* (1), 3469.
- (19) Schenkmyerova, A.; Pinto, G. P.; Toul, M.; Marek, M.; Hernychova, L.; Planas-Iglesias, J.; Daniel Liskova, V.; Pluskal, D.; Vasina, M.; Emond, S.; Dörr, M.; Chaloupkova, R.; Bednar, D.; Prokop, Z.; Hollfelder, F.; Bornscheuer, U. T.; Damborsky, J. Engineering the protein dynamics of an ancestral luciferase. *Nat. Commun.* **2021**, *12* (1), 3616.
- (20) Toth-Petroczy, A.; Tawfik, D. S. Protein Insertions and Deletions Enabled by Neutral Roaming in Sequence Space. *Mol. Biol. Evol.* **2013**, *30* (4), 761–771.
- (21) Rockah-Shmuel, L.; Toth-Petroczy, A.; Sela, A.; Wurtzel, O.; Sorek, R.; Tawfik, D. S. Correlated Occurrence and Bypass of Frame-Shifting Insertion-Deletions (InDels) to Give Functional Proteins. *PLoS Genet.* **2013**, *9* (10), No. e1003882.
- (22) Tawfik, D. S. Loop grafting and the origins of enzyme species. *Science* **2006**, *311* (5760), 475–476.
- (23) Seibert, C. M.; Raushel, F. M. Structural and catalytic diversity within the amidohydrolase superfamily. *Biochemistry* **2005**, *44* (17), 6383–6391.
- (24) Cole, M. F.; Gaucher, E. A. Exploiting Models of Molecular Evolution to Efficiently Direct Protein Engineering. *J. Mol. Evol.* **2011**, *72* (2), 193–203.
- (25) Chen, F.; Gaucher, E. A.; Leal, N. A.; Hutter, D.; Havemann, S. A.; Govindarajan, S.; Ortlund, E. A.; Benner, S. A. Reconstructed evolutionary adaptive paths give polymerases accepting reversible terminators for sequencing and SNP detection. *Proc. Natl. Acad. Sci. USA* **2010**, *107* (5), 1948–1953.
- (26) Liu, G. F.; Cheng, T. T.; Chu, J. L.; Li, S.; He, B. F. Efficient Synthesis of Purine Nucleoside Analogs by a New Trimeric Purine Nucleoside Phosphorylase from *Aneurinibacillus migulanus* AM007. *Molecules* **2019**, *25* (1), 100.
- (27) Erion, M. D.; Stoeckler, J. D.; Guida, W. C.; Walter, R. L.; Ealick, S. E. Purine Nucleoside Phosphorylase. 2. Catalytic Mechanism. *Biochemistry* **1997**, *36* (39), 11735–11748.
- (28) Caradoc-Davies, T. T.; Cutfield, S. M.; Lamont, I. L.; Cutfield, J. F. Crystal structures of *Escherichia coli* uridine phosphorylase in two native and three complexed forms reveal basis of substrate specificity, induced conformational changes and influence of potassium. *J. Mol. Biol.* **2004**, *337* (2), 337–354.
- (29) Wang, M. L.; Cao, R. Y.; Zhang, L. K.; Yang, X. L.; Liu, J.; Xu, M. Y.; Shi, Z. L.; Hu, Z. H.; Zhong, W.; Xiao, G. F. Remdesivir and chloroquine effectively inhibit the recently emerged novel coronavirus (2019-nCoV) in vitro. *Cell Res.* **2020**, *30* (3), 269–271.
- (30) Meanwell, M.; Silverman, S. M.; Lehmann, J.; Adluri, B.; Wang, Y.; Cohen, R.; Campeau, L. C.; Britton, R. A short de novo synthesis of nucleoside analogs. *Science* **2020**, *369* (6504), 725–730.
- (31) Forli, S.; Huey, R.; Pique, M. E.; Sanner, M. F.; Goodsell, D. S.; Olson, A. J. Computational protein-ligand docking and virtual drug screening with the AutoDock suite. *Nat. Protoc.* **2016**, *11* (5), 905–919.
- (32) Liu, G. F.; Tong, X.; Wang, J. L.; Wu, B.; Chu, J. L.; Jian, Y. C.; He, B. F. Reshaping the binding pocket of purine nucleoside phosphorylase for improved production of 2-halogenated-2'-deoxyadenosines. *Catal. Sci. Technol.* **2021**, *11* (13), 4439–4446.